**THE EUROPEAN
PHYSICAL JOURNAL B**

Renormalized parameters for impurity models

A.C. Hewson[1], A. Oguri[2], and D. Meyer[1,a]

[1] Department of Mathematics, Imperial College, London SW7 2BZ, UK
[2] Department of Material Science, Osaka City University, Sumiyoshi-ku, Osaka 558-8585, Japan

Abstract. We show that the low energy behaviour of quite diverse impurity systems can be described by a single renormalized Anderson model, with three parameters, an effective level $\tilde{\epsilon}_d$, an effective hybridization $\tilde{V}$, and a quasiparticle interaction $\tilde{U}$. The renormalized parameters are calculated as a function of the bare parameters for a number of impurity models, including those with coupling to phonons and a Falikov-Kimball interaction term. In the model with a coupling to phonons we determine where the interaction of the quasiparticles changes sign as a function of the electron-phonon coupling. In the model with a Falikov-Kimball interaction we show that to a good approximation the low energy behaviour corresponds to that of a bare Anderson model with a shifted impurity level.

PACS. 75.20.Hr Local moment in compounds and alloys; Kondo effect, valence fluctuations, heavy fermions – 71.10.-w Theories and models of many-electron systems – 71.27.+a Strongly correlated electron systems; heavy fermions

1 Introduction

The low energy behaviour of impurities in a metallic host can be calculated using a numerical renormalization group (NRG) approach in which the higher energy states are progressively eliminated [1,2]. The low temperature thermodynamics of the impurity are deduced from the leading corrections to the low energy fixed point of the renormalization group transformation. An alternative renormalization approach is the renormalized perturbation theory (RPT), as developed originally for field theoretical calculations in quantum electrodynamics (QED) [3]. This technique, with the introduction of counter terms, allows one to by-pass infinities in QED associated with the lack of a high energy cut-off and perform calculations in terms of a renormalized version of the same model. The renormalized parameters are then determined from experiment. This technique is quite general and is not simply about cancellation of infinities, but more about working with parameters appropriate to the energy regime that is being investigated. When this approach is applied to the Anderson impurity model, the effective low energy model generated is just a version of the Anderson model with renormalized parameters. The renormalized perturbation diagrams to second order give the exact low temperature behaviour of the model, which in the Kondo regime can be expressed in terms of a single renormalized parameter, the Kondo temperature T_K [4,5].

In this paper we will clarify the relation between these two renormalization group approaches, and consider the various possible ways of determining the renormalized parameters. We will also generalize the approach to include models which have a coupling to phonons and a Falikov-Kimball screening interaction between the impurity and conduction electrons.

The Anderson model [6] has the form,

$$H_{\mathrm{AM}} = \sum_\sigma \epsilon_d d_\sigma^\dagger d_\sigma + U n_{d,\uparrow} n_{d,\downarrow} + \sum_{k,\sigma} \epsilon_{k,\sigma} c_{k,\sigma}^\dagger c_{k,\sigma}$$
$$+ \sum_{k,\sigma} \left(V_k d_\sigma^\dagger c_{k,\sigma} + V_k^* c_{k,\sigma}^\dagger d_\sigma \right). \tag{1}$$

It describes a localized level ϵ_d of an impurity, hybridized with the conduction electrons of the host metal via the matrix element V_k. There is in addition a local interaction U between the electrons on the impurity site. When $U = 0$ the local level broadens into a resonance, corresponding to a localized quasi-bound state, whose width depends on the quantity $\Delta(\omega) = \pi \sum_k |V_k|^2 \delta(\omega - \epsilon_k)$. It is usual to consider the case of a wide conduction band with a flat density of states where $\Delta(\omega)$ becomes independent of ω and can be taken as a constant Δ.

We briefly review those results of the RPT as applied to the Anderson model which we will need in this paper [4,5]. Here, the renormalized model is characterized by an effective energy level at $\tilde{\epsilon}_d$, and an effective resonance width $\tilde{\Delta}$. Expressions for these renormalized parameters can be derived in terms of the 'bare' parameters, ϵ_d, Δ,

[a] e-mail: `d.meyer@ic.ac.uk`

the local self-energy $\Sigma_\sigma(\omega, h)$ and its frequency derivative $\Sigma_\sigma'(\omega, h)$ evaluated at zero frequency $\omega = 0$, zero magnetic field $h = 0$, and $T = 0$. They are given by

$$\tilde{\epsilon}_d = z(\epsilon_d + \Sigma_\sigma(0,0)), \quad \tilde{\Delta} = z\Delta, \tag{2}$$

where z, the wavefunction renormalization factor, is given by $z = 1/(1 - \Sigma_\sigma'(0,0))$. The effective local interaction $\tilde{U}$ is expressed in terms of the local four-vertex $\Gamma_{\uparrow,\downarrow}(\omega_1, \omega_2, \omega_3, \omega_4)$ evaluated at zero frequency $(\omega_1 = \omega_2 = \omega_3 = \omega_4 = 0)$,

$$\tilde{U} = z^2 \Gamma_{\uparrow,\downarrow}(0,0,0,0). \tag{3}$$

The renormalized effective model has the same form as (1), but in terms of renormalized parameters, and the interaction term is normal-ordered, as it only comes into play when two or more excitations are created relative to the ground state of the interacting system,

$$\tilde{H}_{\mathrm{AM}} = \sum_\sigma \tilde{\epsilon}_d d_\sigma^\dagger d_\sigma + \tilde{U} : n_{d,\uparrow} n_{d,\downarrow} : + \sum_{k,\sigma} \epsilon_{k,\sigma} c_{k,\sigma}^\dagger c_{k,\sigma}$$
$$+ \sum_{k,\sigma} \left(\tilde{V}_k d_\sigma^\dagger c_{k,\sigma} + \tilde{V}_k^* c_{k,\sigma}^\dagger d_\sigma \right), \tag{4}$$

where the colon brackets indicate that the expression within them must be normal-ordered. This renormalized model is similar to that used in earlier phenomenological local Fermi-liquid theories [7], but here it also includes a quasiparticle interaction term.

In the renormalized perturbation theory the Hamiltonians of the bare and renormalized Anderson models are related via $H_{\mathrm{AM}} = \tilde{H}_{\mathrm{AM}} + \tilde{H}_c$, where $\tilde{H}_c$ is the counter-term Hamiltonian given by

$$\tilde{H}_c = \sum_\sigma \lambda_1 d_\sigma^\dagger d_\sigma + \lambda_2 n_{d,\uparrow} n_{d,\downarrow}. \tag{5}$$

The renormalized perturbation expansion is in powers of the renormalized interaction $\tilde{U}$, but all the terms in (4) and (5) are taken into account; the parameters λ_1 and λ_2, and a rescaling factor λ_3, are determined by the condition that there is no further renormalization of the already fully renormalized parameters, $\tilde{\epsilon}_d$, $\tilde{\Delta}$ and $\tilde{U}$ arising from the expansion (the procedure is clearer in the Lagrangian formulation, for details see [5]). The first order expressions for the impurity spin and charge susceptibilities, $\chi_{s,\mathrm{imp}}$ and $\chi_{c,\mathrm{imp}}$ at $T = 0$ derived from the renormalized model are exact [8] and given by

$$\chi_{s,\mathrm{imp}} = \frac{1}{2} \tilde{\rho}_{\mathrm{imp}}(0) \left(1 + \tilde{U} \tilde{\rho}_{\mathrm{imp}}(0) \right), \tag{6a}$$

$$\chi_{c,\mathrm{imp}} = \frac{1}{2} \tilde{\rho}_{\mathrm{imp}}(0) \left(1 - \tilde{U} \tilde{\rho}_{\mathrm{imp}}(0) \right), \tag{6b}$$

where the spin susceptibility is given in units of $(g\mu_B)^2$ and the charge susceptibility differs by a factor of $\frac{1}{4}$ from the usual definition, so it is the isospin equivalent

of $\chi_{s,\mathrm{imp}}$. The quasiparticle density of states at the Fermi level $\tilde{\rho}_{\mathrm{imp}}(0)$ is given by

$$\tilde{\rho}_{\mathrm{imp}}(0) = \frac{\tilde{\Delta}/\pi}{\tilde{\epsilon}_d^2 + \tilde{\Delta}^2}. \tag{7}$$

Exact results for specific heat coefficient γ_{imp} and the occupation of the impurity level $n_{\mathrm{imp},\sigma}$ are

$$\gamma_{\mathrm{imp}} = \frac{2\pi^2}{3} \tilde{\rho}_{\mathrm{imp}}(0), \tag{8}$$

and

$$n_{\mathrm{imp},\sigma} = \frac{1}{2} - \frac{1}{\pi} \tan^{-1} \left(\frac{\tilde{\epsilon}_d}{\tilde{\Delta}} \right), \tag{9}$$

which corresponds to the Friedel sum rule [9]. These two results correspond to a local Fermi-liquid theory with non-interacting quasiparticles and can be deduced from the zero order ($\tilde{U} = 0$) renormalized model. The temperature dependence of the impurity contribution to the conductivity $\sigma(T)$ has also been calculated for the symmetric model to order T^2 from the renormalized self-energy calculated to second order in $\tilde{U}$. The result is

$$\sigma(T) = \sigma_0 \left\{ 1 + \frac{\pi^2}{3} \left(\frac{T}{\tilde{\Delta}} \right)^2 \left[1 + 2 \left(\frac{\tilde{U}}{\pi\tilde{\Delta}} \right)^2 \right] + \mathrm{O}(T^4) \right\}. \tag{10}$$

When the renormalized parameters are expressed in terms of the self-energy and the vertex function these results coincide with the exact expressions derived by Yamada [10] from an analysis of perturbation theory to all orders U, and the Fermi-liquid results of Nozières [11] in the Kondo limit. This result has also been generalized to include the leading non-linear correction to the differential conductance through a quantum dot in the Fermi liquid regime [12], which is of order V_e^2, where voltage V_e is the voltage difference across the dot. In the localized or Kondo limit the renormalized parameters can be reduced to one single parameter, the Kondo temperature T_K. For $U \gg |\epsilon_d|$, and $\epsilon_d \ll 0$, the electron in the d-state at the impurity site will be localized and as a consequence the impurity charge susceptibility must vanish in this limit. From equations (6) and (9), this implies $\tilde{U} = \pi\tilde{\Delta}$ and $\tilde{\epsilon}_d = 0$. If the impurity susceptibility at $T = 0$ is expressed in terms of a Kondo temperature T_K defined by $\chi_{s,\mathrm{imp}} = 1/4T_K$, then the renormalized parameters can be expressed in terms of a single energy scale T_K, so $\tilde{U} = \pi\tilde{\Delta} = 4T_K$, and the Wilson or χ/γ ratio, $R = 1 + \tilde{U}\tilde{\rho}_d(0) = 2$ [11].

It is clear that the renormalized Anderson model derived in the RPT must be directly related to the low energy effective model obtained in the numerical renormalization group (NRG) calculations by Wilson [1] for the s-d (Kondo) model, and by Krishnamurthy, Wilkins and Wilson (KWW) [2] for the Anderson model. The RPT and NRG approaches are, however, rather different. In the Wilson approach the conduction band of the Anderson model is replaced by a discrete spectrum of states, which is then expressed in the form of a tight-binding chain with the impurity at one end. The Hamiltonian for the discrete

model for a finite chain with $N + 2$ sites, including the impurity site, is

$$H_{\mathrm{AM}}^N = \sum_\sigma \epsilon_d d_\sigma^\dagger d_\sigma + U n_{d,\uparrow} n_{d,\downarrow} + V \sum_\sigma \left(d_\sigma^\dagger c_{0,\sigma} + c_{0,\sigma}^\dagger d_\sigma \right)$$
$$+ \sum_{n=0,\sigma}^{n=N} \Lambda^{-n/2} \xi_n \left(c_{n,\sigma}^\dagger c_{n+1,\sigma} + c_{n+1,\sigma}^\dagger c_{n,\sigma} \right), \quad (11)$$

where $\Lambda > 1$ is the discretization parameter, and ξ_n is given by

$$\xi_n = \frac{D}{2} \frac{\left(1 + \Lambda^{-1}\right)\left(1 - \Lambda^{-n-1}\right)}{\left(1 - \Lambda^{-2n-1}\right)^{1/2}\left(1 - \Lambda^{-2n-3}\right)^{1/2}}, \quad (12)$$

and $2D$ is the width of the conduction band [1]. The discretization of the conduction band is logarithmic and such that the density of levels increases as the Fermi-level is approached, and $\epsilon = 0$ is the limit point of the sequence. The model is then solved by iterative diagonalization, and when the matrices get too large, the Hibert space is truncated such that 500–1500 of the lowest lying energy states are retained at each step and the higher energy states are neglected. As the couplings along the chain fall off as $\Lambda^{-n/2}$, where n is the nth site as $\Lambda > 1$, lower and lower energy scales are reached. The Hamiltonian however is rescaled after each step by a factor $\Lambda^{1/2}$ so that the lowest energy scale is formally the same after each iteration.

A renormalization group transformation can be set up in which the states and couplings can be compared after each step. This renormalization group transformation for the s-d (Kondo) and Anderson model has a low energy fixed point corresponding to states of a free chain uncoupled from the impurity. In the s-d case this was interpreted as a $J \to \infty$ fixed point [1], and for the Anderson a $V \to \infty$ fixed point [2], so that the impurity and first site become essentially uncoupled from the chain. As this fixed point Hamiltonian corresponds to a free chain it gives no finite contribution to the impurity susceptibility and specific heat. However, as the low temperature behaviour of this model corresponds to a Fermi-liquid it is more appropriate to base the interpretation of the fixed point in terms of an Anderson model with a finite V. There is then a 1-1 correspondence of the excitations of the interacting system with those of the non-interacting model $U = 0$, which is a feature of Fermi liquid theory. It also allows one to make a direct connection with the renormalized perturbation approach to calculate the three renormalized parameters, $\tilde{\Delta}$, $\tilde{\epsilon}_d$ and $\tilde{U}$. A knowledge of how these renormalized parameters, such as the quasiparticle interaction $\tilde{U}$, depend on the bare parameters of the model can give us considerable insight into the low energy behaviour of impurity systems, and leads immediately to the quasiparticle density of states from equation (7). Substitution into the other RPT results gives the low temperature thermodynamic and response functions, including the temperature dependence of the conductivity.

In the next section of this paper we give a new way of analysing the fixed point which leads directly to the relevant renormalized parameters, and is applicable to systems with a non-symmetric and non-constant density of states. The approach is then applied to generalizations of the model to include an interaction with phonons, and Falikov-Kimball terms, for which there are in general no exact results. The approach can be extended to more general impurity models including orbital degeneracy [15].

2 Calculation of renormalized parameters

In this section we will examine the low energy NRG fixed point of the Anderson model as a renormalized version of the same model and deduce the renormalized parameters $\tilde{\epsilon}_d$, $\tilde{\Delta}$ and $\tilde{U}$. The starting point of the NRG calculation is the discretized form of the model given in equation (11). The many-body states are calculated using the iteration procedure as outlined in the previous section. For a given N, we denote the minimum energy required to add a single electron to the ground state by $E_p(N)$, and and the minimum energy to create a single hole by $E_h(N)$. If these single particle and hole excitations correspond to a renormalized Anderson model, then asymptotically they should coincide with those of the free model with an appropriate choice of $\tilde{\epsilon}_d$ and $\tilde{\Delta}$ (the term in $\tilde{U}$ plays a role only when more than one single particle excitation is created from the ground state). This problem is considered in the appendix where we define N-dependent quantities, $\tilde{\epsilon}_d(N)$, and $\tilde{\Delta}(N) = \pi \tilde{V}(N)^2/2$, via the two equations,

$$\frac{\pi E_p(N)\Lambda^{-(N-1)/2}}{2\tilde{\Delta}(N)} - \frac{\pi\tilde{\epsilon}_d(N)}{2\tilde{\Delta}(N)} = \Lambda^{(N-1)/2} g_{00}(E_p(N)), \quad (13)$$

$$\frac{-\pi E_h(N)\Lambda^{-(N-1)/2}}{2\tilde{\Delta}(N)} - \frac{\pi\tilde{\epsilon}_d(N)}{2\tilde{\Delta}(N)} = \Lambda^{(N-1)/2} g_{00}(-E_h(N)), \quad (14)$$

where $g_{00}(\omega)$ is the local Green's function for the site $n = 0$ on the conduction electron chain in Hamiltonian (11) in the absence of the impurity ($V = 0$, see appendix). The renormalized parameters $\tilde{\epsilon}_d$ and $\tilde{\Delta}$ corresponding to the low energy fixed point are given by $\tilde{\epsilon}_d = \lim_{N\to\infty} \tilde{\epsilon}_d(N)$ and $\tilde{\Delta} = \lim_{N\to\infty} \tilde{\Delta}(N)$ and are given by equations (40) and (41) in the appendix.

In Figure 1 we plot the quantities $\tilde{\Delta}(N)$ and $\tilde{\epsilon}_d(N)$ against N for a model with $U/\pi\Delta = 6.0$ and $\epsilon_d/\pi\Delta = -4.0$. For the impurity site $N = 0$ we take $\tilde{\Delta}(0) = \Delta$, and $\tilde{\epsilon}_d(0)$ to be the average Hartree-Fock value $\epsilon_d + U n_d/2$, where n_d is the total occupation value at the impurity site, calculated within the Hartree-Fock theory. This Hartree-Fock value for $\tilde{\epsilon}_d(0)$ is considerably shifted from the bare value ϵ_d, but clearly fits the trend in values for $\tilde{\epsilon}_d(N)$ for small N. If the one-particle excitations can be described by an effective non-interacting Anderson model then $\tilde{\Delta}(N)$ and $\tilde{\epsilon}_d(N)$ should be independent of N. This can indeed seen to be the case for $N > 40$ so for this range these excitations can be described by a model with renormalized parameters $\tilde{\Delta}$ and $\tilde{\epsilon}_d$. As the bare parameters correspond to a model in the Kondo regime one sees that in
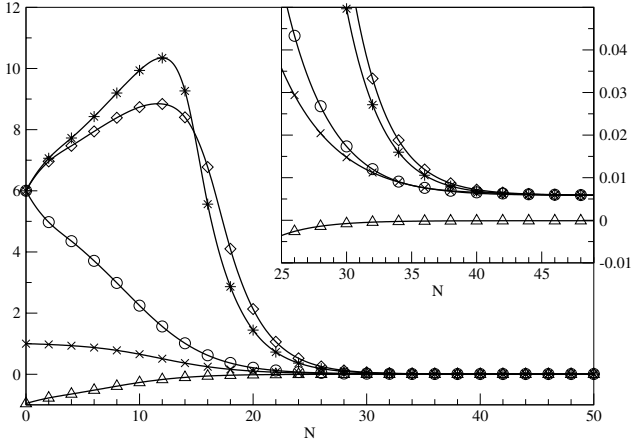
Fig. 1. Plots of the parameters, $\tilde{\Delta}(N)/\pi\Delta$ (crosses), $\tilde{\epsilon}_d(N)/\pi\Delta$ (triangles), $\tilde{U}_{pp}(N))/\pi\Delta$ (diamonds), $\tilde{U}_{hh}(N)/\pi\Delta$ (stars) and $\tilde{U}_{ph}(N)/\pi\Delta$ (circles), for the model with bare parameters, $U/\pi\Delta = 6.0$ and $\epsilon_d/\pi\Delta = -4.0$. The inset shows the results for $N > 25$ on a higher resolution energy scale (see right hand scale).

this case $\tilde{\epsilon}_d \approx 0$, whereas $\tilde{\Delta}/\Delta$ is small but finite, $\tilde{\Delta}$ being of the order of the Kondo temperature T_K.

Once the renormalized parameters $\tilde{\epsilon}_d$ and $\tilde{V}$ have been determined the free quasiparticle Hamiltonian can be diagonalized and written in the form

$$\Lambda^{-(N-1)/2} \sum_{k=1}^{(N+2)/2} \left(E_{p,k}(N)p_{k,\sigma}^{\dagger}p_{k,\sigma} + E_{h,k}(N)h_{k,\sigma}^{\dagger}h_{k,\sigma} \right), \tag{15}$$

where $p_{k,\sigma}^{\dagger}$, $p_{k,\sigma}$, and $h_{k,\sigma}^{\dagger}$, $h_{k,\sigma}$, are the creation and annihilation operators for the quasiparticle and quasihole excitations, and $\Lambda^{-(N-1)/2}E_{p,k}(N)$ and $\Lambda^{-(N-1)/2}E_{h,k}(N)$ are the corresponding excitation energies relative to the ground or vacuum state $|0\rangle$; the scale factor $\Lambda^{-(N-1)/2}$ is due to the fact that the energies are calculated for the rescaled Hamiltonian, which is such that $E_{p,k}(N)$ and $E_{h,k}(N)$ for $k = 1$ are of order 1. For the lowest-lying particle and hole levels, we have $E_p(N) = E_{p,1}(N)$ and $E_h(N) = E_{h,1}(N)$.

From the parameters, $\tilde{\epsilon}_d$ and $\tilde{\Delta}$, which determine the free quasiparticle excitations we can immediately deduce the occupation of the impurity level n_{imp} at $T = 0$ from equation (9), which depends only on the ratio $\tilde{\epsilon}_d/\tilde{\Delta}$, the quasiparticle density of states from (7), and the impurity specific heat coefficient γ_{imp} from (8).

To calculate the spin and charge susceptibilities and the low temperature dependence of the conductivity we need to include a quasiparticle interaction term, which for the rescaled model takes the form,

$$H^U(N) = \tilde{U}\Lambda^{(N-1)/2} : d_{\uparrow}^{\dagger}d_{\uparrow}d_{\downarrow}^{\dagger}d_{\downarrow} : \tag{16}$$

Asymptotically as $N \to \infty$ the effect of this term on the low-lying many-particle excitations tends to zero so it is sufficient to calculate the effect of this term to first order in $\tilde{U}$. To this end we need the operator d_{σ} expressed in

terms of the eigenstates of (15),

$$d_{\sigma} = \sum_{k=1}^{(N+2)/2} \left(\psi_{p,k}(-1)p_{k\sigma} + \psi_{h,k}(-1)h_{k\sigma}^{\dagger} \right). \tag{17}$$

If the lowest two-particle excitation from the ground state for the interacting system for a given N has an energy $E_{pp}(N)$, then we can calculate $\tilde{U}$ by equating the energy difference $E_{pp}(N) - 2E_p(N)$ to that calculated using (16) asymptotically in the limit $N \to \infty$. For finite N we can use this equation to define an N-dependent renormalized interaction $\tilde{U}_{pp}(N)$,

$$E_{pp}(N) - 2E_p(N)$$
$$= \tilde{U}(N)\Lambda^{(N-1)/2} \left| \psi_{p,1}^*(-1) \right|^2 \left| \psi_{p,1}^*(-1) \right|^2, \tag{18}$$

where $|\psi_{p,1}(-1)|^2$ is given by

$$|\psi_{p,1}|^2 = \frac{1}{1 - \tilde{V}^2(N)\Lambda^{(N-1)}g'_{00}(E_p(N))} \tag{19}$$

where $g'_{00}(\omega)$ is the derivative of $g_{00}(\omega)$.

Alternatively we could consider the same procedure for a two hole excitation $E_{hh}(N)$ and in a similar way define an N-dependent renormalized interaction $\tilde{U}_{hh}(N)$, or a particle-hole excitation $E_{ph}(N)$ to define a renormalized interaction $\tilde{U}_{ph}(N)$. In this latter case, as a positive U leads to particle-hole attraction, we use $E_p(N) + E_h(N) - E_{ph}(N)$ on the left-hand side of equation (18).

If these two-particle excitations can be described by an effective Anderson model then $\tilde{U}_{pp}(N)$, $\tilde{U}_{hh}(N)$ and $\tilde{U}_{ph}(N)$ should be independent of N and also independent of the particle-hole labels. In Figure 1 we also plot $\tilde{U}_{pp}(N)$, $\tilde{U}_{hh}(N)$ and $\tilde{U}_{ph}(N)$ as a function of N for the parameters used earlier, $U/\pi\Delta = 6$ and $\epsilon_d/\pi\Delta = -4$, with values at $N = 0$ corresponding to the unrenormalized interaction U. We see that for $N > 40$ the values of $\tilde{U}_{pp}(N)$, $\tilde{U}_{hh}(N)$ and $\tilde{U}_{ph}(N)$ do coincide and become independent of N so for the low energy excitations one can define a unique renormalized interaction via $\tilde{U} = \lim_{N\to\infty} \tilde{U}_{\alpha,\alpha'}(N)$, where $\alpha, \alpha' = p, h$. What is more, because the model with these chosen parameters corresponds to the Kondo regime, the value of $\tilde{U}$ coincides with the value of $\pi\tilde{\Delta}$, clearly seen in the inset in Figure 1, and as can be deduced from equation (6) for $\chi_{c,\mathrm{imp}} = 0$.

2.1 Results for symmetric model

The estimates of $\tilde{\Delta}$ and $\tilde{U}$ for the symmetric model can be checked indirectly from the exact Bethe ansatz results for this model [13,14]. The exact RPT results for the impurity spin susceptibility and specific heat coefficient at $T = 0$ for the symmetric model from (6) and (8) are

$$\chi_{s,\mathrm{imp}} = \frac{1}{2\pi\tilde{\Delta}}\left(1 + \frac{\tilde{U}}{\pi\tilde{\Delta}}\right), \quad \gamma_{\mathrm{imp}} = \frac{2\pi}{3\tilde{\Delta}}. \tag{20}$$

Table 1. The renormalized parameters for the symmetric Anderson model for $U/\pi\Delta = 1.0$ and $U/\pi\Delta = 2.0$ calculated using the NRG and different values of the discretization parameter Λ. These results are compared with the corresponding values deduced from exact Bethe ansatz results.

NRG	$U/\pi\Delta = 1$			$U/\pi\Delta = 2$		
	$\tilde{\Delta}/\Delta$	$\tilde{U}/\pi\Delta$	R	$\tilde{\Delta}/\Delta$	$\tilde{U}/\pi\Delta$	R
$\Lambda = 2.0$	0.6288	0.4779	1.7600	0.2389	0.2298	1.9620
$\Lambda = 2.5$	0.6287	0.4777	1.7599	0.2390	0.2300	1.9621
$\Lambda = 3.0$	0.6288	0.4780	1.7601	0.2390	0.2299	1.9619
$\Lambda = 3.5$	0.6288	0.4780	1.7601	0.2390	0.2299	1.9620
Exact (BA)	0.6289	0.4780	1.7601	0.2392	0.2301	1.9620

By equating these to $\chi_{s,\mathrm{imp}}$ and γ_{imp} from the Bethe ansatz we can deduce $\tilde{\Delta}$ and $\tilde{U}$.

Though the discrete model (11) with $\Lambda > 1$ and the original model (1) with a continuous spectrum have essentially the same low energy spectrum, the models are not identical. The dependence of the renormalized parameters on the parameters of the bare model may differ, and for the discrete model there is a dependence on Λ. Such differences can occur in calculations where the high energy excitations, or high cut-offs, are treated differently. This situation occurs for the N-fold degenerate models ($U = \infty$) where the imposition of the high energy cut-off D' in the Bethe ansatz calculations for the linear dispersion model differs from the band width D for the conventional model, but a relation between these cut-offs can be found such that the results from the Bethe ansatz calculations can be translated into those for the conventional model [16]. A similar situation applies here. The results can be made equivalent by replacing the bandwidth D of the discrete model by DA_Λ, with A_Λ given by

$$A_\Lambda = \frac{1}{2}\frac{1 + \Lambda^{-1}}{1 - \Lambda^{-1}}\ln\Lambda, \qquad (21)$$

where $A_\Lambda \to 1$ in the continuum limit $\Lambda \to 1$. This result, which is given in the paper of KWW [2] and also used in the paper of Sakai, Shimizu and Kasuya [18], is derived by the requirement that the low energy spectrum of the discrete and continuum model coincide for $U = 0$. It means that V^2 must be increased by a factor A_Λ when making a comparison with the results of a continuum model with a given $U/\pi\Delta$.

The values of the renormalized parameters $\tilde{\Delta}$, $\tilde{U}$ and the χ/γ or Wilson ratio, $R = 1 + \tilde{U}/\pi\tilde{\Delta}$ [1,2], deduced from these are shown in Table 1, where they are compared with those deduced from the Bethe ansatz results. The agreement with the Bethe ansatz results is remarkably good, with errors only of the order of 0.1%, even for values of Λ as large as 3.5. It is important for such accurate agreement, particularly for larger values of Λ that the A_Λ factor is taken into account.

In Figure 2 we make a more extensive comparison of the results for $\tilde{\Delta}$ and $\tilde{U}$ deduced from the NRG calculations and those deduced from the Bethe ansatz for both positive and negative values of U. The agreement is excellent over the whole range. For $U/\pi\Delta > 2$ the energy
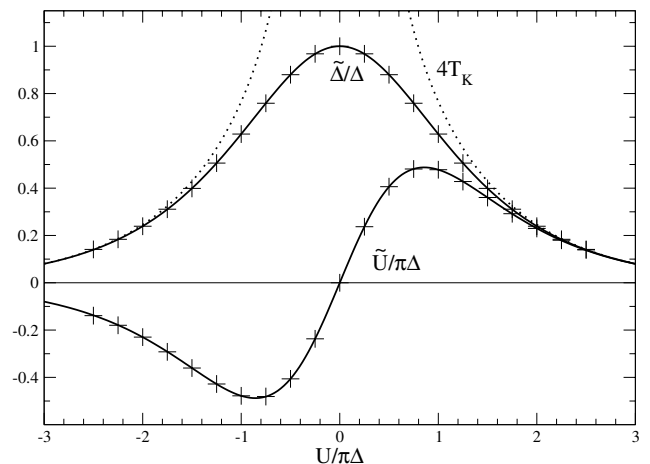
Fig. 2. Renormalized parameters $\tilde{U}/\pi\Delta$ and $\tilde{\Delta}/\Delta$ as a function of $U/\pi\Delta$. The two curves are the results deduced from the Bethe ansatz, and the points marked with a cross are those deduced from NRG calculations with $\Lambda = 2.0$. For $|U|/\pi\Delta > 2.0$ the two energy scales merge and asymptotically approach $4T_K$ (dotted line), where T_K is the Kondo temperature.

scales merge as the impurity charge becomes localized (Kondo regime) and the impurity charge susceptibility tends to zero. In this limit $\tilde{U}/\pi\tilde{\Delta} \to 1$ and as a consequence the Wilson ratio $R \to 2$. The single renormalized energy scale in this regime is the Kondo temperature T_K, and $\pi\tilde{\Delta} = \tilde{U} = 4T_K$. In the negative U regime such that $U/\pi\Delta < -2$ a local bipolaron forms such that the spin susceptibility tends to zero, and the charge susceptibility is enhanced by a factor of 2. In this limit the energy scales again merge such that $\tilde{U}/\pi\tilde{\Delta} \to -1$. This is because a Kondo effect develops in the isospin channel (doubly occupancy of the impurity site corresponding to up-isospin, and zero occupancy to down-isospin), such that $\pi\tilde{\Delta} = -\tilde{U} = 4T_K$, as the real spin fluctuations are suppressed and $\chi_{s,\mathrm{imp}} \to 0$. There is a possibility that a Kondo effect of this type might be seen in degenerate atomic gases with the doubly occupied paired states corresponding to molecules [17]. The general expression for T_K that covers both Kondo regimes is

$$T_K = |U|\left(\frac{\Delta}{2|U|}\right)^{1/2} e^{-\pi|U|/8\Delta + \pi\Delta/2|U|}. \qquad (22)$$

The analysis of the irrelevant terms about the fixed point is not the only way to deduce some of the renormalized parameters from the NRG calculations. If the NRG approach is used also to calculate the dynamics of the impurity model [19,20] then $\tilde{\epsilon}_d$ and $\tilde{\Delta}$ can be deduced from the self-energy and its derivative for $\omega = 0$ and substituted in equation (2). Typical values for $\tilde{\Delta}$ calculated in this way for the symmetric model ($\tilde{\epsilon}_d = 0$) for $U/\pi\Delta = 1$ and $U/\pi\Delta = 2$ are 0.6155 and 0.2350, respectively for $\Lambda = 2$. They compare well with the Bethe ansatz values given in Table 1. The errors are greater than those deduced from the analysis of the fixed point, of the order of 2–3%, but still quite small, and are of the order to be expected in the calculation of dynamical quantities. Unfortunately the evaluation of $\tilde{U}$ from equation (3) requires a knowledge of the four-vertex $\Gamma_{\uparrow,\downarrow}(0,0,0,0)$ which is very difficult to calculate directly from an NRG calculation, as it involves the Fourier transform of the two-particle Green's function with respect to three independent frequency parameters. Both $\tilde{\Delta}$ and $\tilde{U}$ have, however, been calculated from equations (2) and (3) from perturbation theory to third order in U for the symmetric model [5], and the results are

$$\tilde{\Delta} = \Delta \left\{ 1 - \left(3 - \frac{\pi^2}{4} \right) \left(\frac{U}{\pi\Delta} \right)^2 + \dots \right\}, \quad (23)$$

and

$$\tilde{U} = U \left\{ 1 - \left(\frac{\pi^2 - 9}{4} \right) \left(\frac{U}{\pi\Delta} \right)^2 + \dots \right\}. \quad (24)$$

These perturbational results are in good agreement with the exact results in the range $U/\pi\Delta < 0.5$; at $U/\pi\Delta = 0.5$ the error in $\tilde{\Delta}$ is less than 1.5% and that for $\tilde{U}$ less than 4%.

We were able to define running renormalized parameters, such as $\tilde{\Delta}(N)$ and $\tilde{\epsilon}_d(N)$ as a function of N, which raises the possibility that they can be translated into effective parameters appropriate for calculations on an energy scale $\omega_N = \eta D \Lambda^{-(N-1)/2}$ or temperature scale, $T_N = \omega_N$, where η is an appropriately chosen constant of order unity. We do not however have a unique value for $\tilde{U}(N)$. Nevertheless, for the particle-hole symmetric case if we take the value of $\tilde{U}_{pp}(N)$ ($=\tilde{U}_{hh}(N)$) as $\tilde{U}(N)$, and translate this, together with $\tilde{\Delta}(N)$ and $\tilde{\epsilon}_d(N)$, into parameters appropriate for a temperature scale T_N, we can generalize the RPT expression for the impurity susceptibility in equation (6) to finite temperatures,

$$\chi_{\text{imp}}(T) = \tilde{\chi}_{\text{imp}}^{(0)}(T) \left(1 + 2\tilde{U} \tilde{\chi}_{\text{imp}}^{(0)}(T) \right), \quad (25)$$

where $\tilde{\chi}_{\text{imp}}^{(0)}(T)$ is the free quasiparticle contribution to the impurity susceptibility given by

$$\tilde{\chi}_{\text{imp}}^{(0)}(T) = -\frac{1}{2} \int_{-\infty}^{\infty} \tilde{\rho}_{\text{imp}}(\omega) \frac{\partial f(\omega)}{\partial \omega} d\omega \quad (26)$$

in units of $(g\mu_B)^2$, where $f(\omega) = 1/(e^{\omega/T}+1)$, and $\tilde{\rho}_{\text{imp}}(\omega)$ is the free quasiparticle density of states given by equation (7). We calculate $\tilde{\chi}_{\text{imp}}^{(0)}(T)$ for the symmetric model in
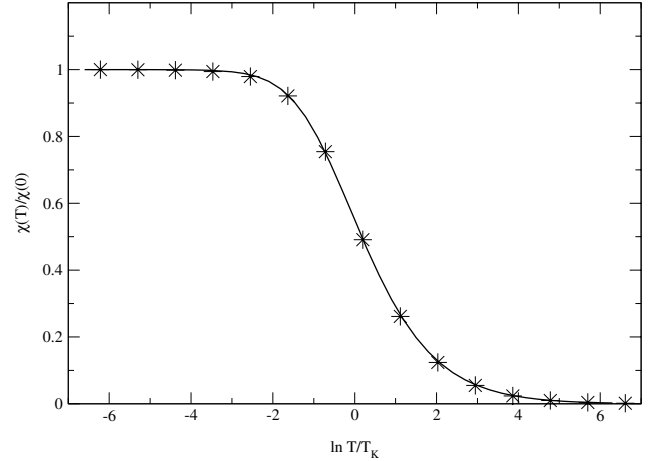

Fig. 3. The temperature dependent impurity susceptibility $\chi_{\text{imp}}(T)/\chi_{\text{imp}}(0)$ (stars) versus $\ln(T/T_K)$ evaluated from equation (25) for the symmetric model for $U/\pi\Delta = 6.0$, compared to the results of the Bethe ansatz solution (continuous curve) for the s-d model given by Tsvelik and Wiegmann [13].

the Kondo regime for $U/\pi\Delta = 6.0$ at values of T_N, using the renormalized parameters $\tilde{\Delta}(T_N)$ and $\tilde{\epsilon}_d(T_N) = 0$ in evaluating the free quasiparticle density of states for this energy scale, with $\eta = 1.2$ as is used in the NRG evaluation of spectral densities on a scale ω_N (see for example [19,20]). We then deduce $\chi_{\text{imp}}(T)$ from equation (25) using $\tilde{U}(T_N)$. In Figure 3 we compare the results of this calculation with the Bethe ansatz results for the s-d model given in reference [13]. There is quite a remarkable agreement with the exact Bethe ansatz results over this temperature range, and the value of $\chi_{\text{imp}}(T)$ in the extreme high temperature range corresponds to that of the free bare model, $1/8T$. The agreement is much less good if we use $\tilde{U}_{ph}(N)$ for $\tilde{U}(N)$ and, as there is not a unique prediction for this quantity, one cannot place too much reliance on this calculation. However, it does suggest that one might be able to define a renormalized perturbation theory with running coupling constants (this is possible in a magnetic field, with field dependent parameters, as we will demonstrate elsewhere).

2.2 Results for asymmetric model

We now consider how the renormalized parameters vary as the bare parameters change from one qualitatively different regime of the model to another. We start first of all with the value $\epsilon_d = -\pi\Delta = $ constant, and then increase U from negative values of U to $U = 2.7\pi\Delta$. This takes us from what might be called the full orbital regime to the Kondo regime. The results are plotted in Figure 4. We see that $\tilde{\epsilon}_d$ increases at first approximately linearly with U until $U/\pi\Delta \sim 1$, and then slowly increases monotonically through zero at the symmetric point $U/\pi\Delta = 2$, remaining very close to zero in the Kondo regime at higher values of U. The renormalized resonance width $\tilde{\Delta}$ decreases monotonically over the same range, though only
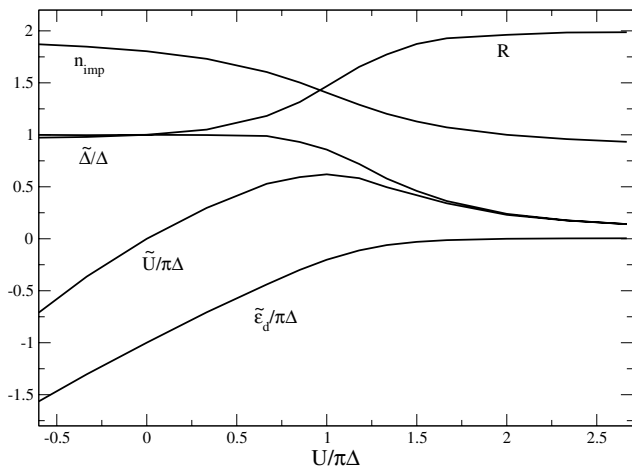
Fig. 4. The renormalized parameters $\tilde{\Delta}/\pi\Delta$, $\tilde{\epsilon}_d/\pi\Delta$, and $\tilde{U}/\pi\Delta$, the Wilson ratio $R = 1 + \tilde{U}\tilde{\rho}_d(0)$, and the impurity occupation value n_{imp} are plotted for the asymmetric Anderson model for a fixed impurity level $\epsilon_d = -\pi\Delta$ as a function $U/\pi\Delta$. Over this range the state of the impurity changes from the full orbital to the Kondo regime.

Fig. 5. Plots of the spectral density $\rho_d(\omega)$ as a function of ω: (i) for values of $\tilde{U}/\pi\Delta$ with $\epsilon_d = -\pi\Delta$ over the same range of values as in Figure 4, and (ii) for values of $\epsilon_d/\pi\Delta$ with $U = 2\pi\Delta$ over the same range as in Figure 6. The heights of the maxima in each case are normalized to unity so that the position of the peak can be compared with the values of $\tilde{\epsilon}_d$ (dotted line) taken from Figure 4 for plot (i), and from Figure 6 for plot (ii). The values of U for the curves in (i) can be read off from the left hand scale from the coordinates of the corresponding maxima, and those for ϵ_d in (ii) from the right hand scale.

slowly at first in the full orbital regime, and approaches zero in the limit $U \to \infty$. The quasiparticle interaction $\tilde{U}$ increases at first linearly with U, reaching a maximum for $U/\pi\Delta \sim 1$, and then decreases so that its energy scale merges with that for $\tilde{\Delta}$, with $\tilde{U} = \pi\tilde{\Delta} = 4T_{\text{K}}$, as for the symmetric model discussed in the previous section. Over the same parameter range n_{imp} decreases from an initial value of 1.8 to slightly below unity at $U = 2.7\pi\Delta$. The Wilson ratio or χ/γ ratio, $R = 1 + \tilde{U}\tilde{\rho}_d(0)$, increases from 1 and asymptotically approaches 2 in the Kondo regime. For negative values of U, $\tilde{\epsilon}_d$ and $\tilde{U}$ decrease linearly as U decreases and $\tilde{\Delta}/\Delta$ approaches unity. In full orbital regime $U/\pi\Delta < 0.5$, including the range with larger negative values of U, the Hartree-Fock theory, where $\tilde{\epsilon}_d = \epsilon_d + Un_d/2$ and $\tilde{\Delta} = \Delta$, constitutes a reasonably good approximation.

It is interesting to compare this behaviour with that for the spectral density $\rho_d(\omega)$ of the d-electron Green's function, which can be calculated from the NRG results. Some of the results for $\rho_d(\omega)$ over the same parameter range are shown in Figure 5(i). Initially there is only a single resonance which moves to higher energies as U is increased. As the Kondo regime is approached this splits into a three peaked structure, the central narrow peak at the Fermi-level being the many-body Kondo resonance. The renormalized Anderson model given by equation (4) describes only a single resonance, but is valid for the low energy behaviour in all the parameter regimes. We see that for smaller values of U, and in the negative U regime, $\tilde{\epsilon}_d$ tracks at first the lower resonance, increasing monotonically, and in the Kondo regime tracks the Kondo resonance. The precise nature of this tracking is made evident in Figure 5(i) where the curve for $\tilde{\epsilon}_d$ taken from Figure 4 is plotted with the spectral density results, where the main peak for each $\rho_d(\omega)$ has been normalized to unity for the comparison; the maxima of these peaks all lie on the curve.
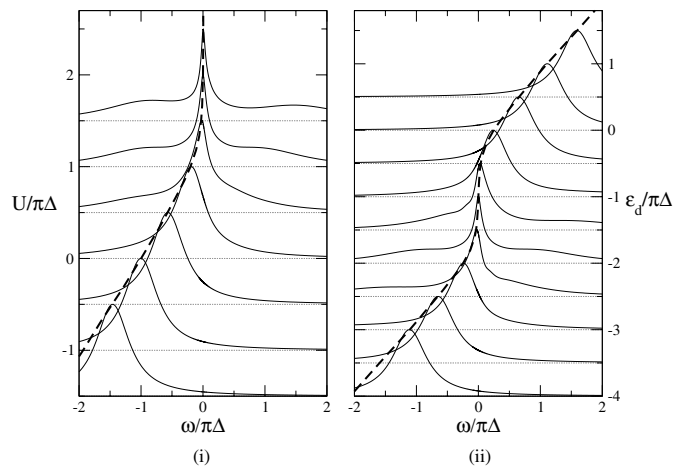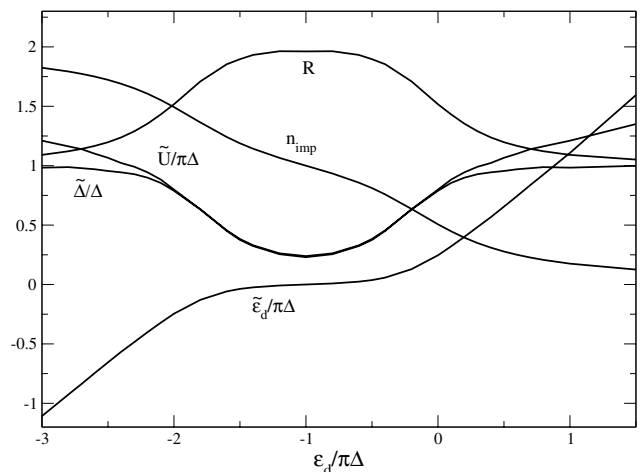

Fig. 6. The renormalized parameters $\tilde{\Delta}/\pi\Delta$, $\tilde{\epsilon}_d/\pi\Delta$, and $\tilde{U}/\pi\Delta$, the Wilson ratio R and the impurity occupation value n_{imp} are plotted for the asymmetric Anderson model for a fixed value $U = 2\pi\Delta$ as a function of $\epsilon_d/\pi\Delta$. On increasing ϵ_d through this range the impurity state passes from the full orbital state, through a mixed valence and Kondo regime, a second mixed valence regime, and to a final empty orbital state.

The height of the atomic-like peaks in this plot, which appear at $\omega \sim \epsilon_d$ and $\omega \sim \epsilon_d + U$ for larger U in the Kondo regime, become somewhat flattened in the normalization as the Kondo peak is so high, making them difficult to see clearly in Figure 5.

In Figure 6 we give the renormalized parameters for a complementary scan. In this case we start first of all with $\epsilon_d = -3\pi\Delta$ and $U = 2\pi\Delta$, which is in the almost full

orbital regime as $\epsilon_d + U < 0$, and then increase ϵ_d with a fixed value for U to a final value $\epsilon_d = 1.5\pi\Delta$. In doing so we move to a mixed valence regime for $\epsilon_d + U \sim 0$, then for $\epsilon_d = -\pi\Delta$ the Kondo regime for the symmetric model with $U/\pi\Delta = 2$, another mixed valence regime for $\epsilon_d \sim 0$, and finally an empty orbital regime for $\epsilon_d > \pi\Delta$. In the earlier renormalization group analysis of KWW [2], these parameter regimes are interpreted in terms of essentially three different fixed points, (i) the full (empty) orbital (ii) the strong coupling and (iii) the mixed valent. In the analysis here, however, they are simply different parameter regimes of a single renormalized Anderson model. We see from Figure 6 the characteristic features of full and empty orbital regimes, $\tilde{\epsilon}_d$ increases linearly with ϵ_d, the Wilson ratio $R \sim 1$, $n_{\mathrm{imp}} \sim 2$ or 0, and $\tilde{\Delta}$ and $\tilde{U}$ are independent energy scales. In contrast in the Kondo regime, $\tilde{\epsilon}_d \approx 0$ and is largely independent of ϵ_d, the Wilson ratio $R \sim 2$, $n_{\mathrm{imp}} \sim 1$, and the energy scales $\tilde{\Delta}$ and $\tilde{U}$ have merged such that $\tilde{U} = \pi\tilde{\Delta}$. The mixed valence regimes appear more as cross-over regions between these two types of behaviour, where the independence of the two energy scales $\tilde{\Delta}$ and $\tilde{U}$ emerges. The curve for $\tilde{\epsilon}_d$ from Figure 6 is plotted in Figure 5(ii) with the corresponding results for the spectral density $\rho_d(\omega)$, with the height of the peaks normalized to unity. The renormalized level $\tilde{\epsilon}_d$ is found to track the single peak in the full orbital regime as it moves up through the intermediate valence regime $\epsilon_d + U \sim 0$, where a second lower peak develops near $\omega \sim \epsilon_d$, and then it tracks the central narrow resonance at the Fermi-level in the Kondo regime, where a third upper peak develops near $\omega \sim \epsilon_d + U$. The reverse process occurs as ϵ_d increases from $\epsilon_d \sim -\pi\Delta$, as the side peaks disappear and a single peak emerges in the empty orbital regime. As in Figure 5(i) atomic-like side peaks at $\omega \sim \epsilon_d$, and $\omega \sim \epsilon_d + U$, which appear in the mixed valence and Kondo regimes, are only just discernable due to the normalization of the height of the central resonance. If we concentrate on the mixed valence regime for $\epsilon_d \sim 0$ in Figure 6, we see that there is a significant upward shift of $\tilde{\epsilon}_d$. This reflects the effective shift in the bare level ϵ_d obtained by Haldane [21] in a poor man's scaling treatment in which the virtual charge fluctuations were eliminated to focus on the mixed valent regime. For the $U = \infty$ limit, the thermodynamic behaviour of the model in this regime was shown by Haldane to depend on the ratio $\bar{\epsilon}_d/\Delta$, where $\bar{\epsilon}_d = \epsilon_d + \Delta/\pi \ln(\pi D/2\Delta)$. For the renormalized Anderson model the equivalent ratio is $\tilde{\epsilon}_d/\tilde{\Delta}$, so $\bar{\epsilon}_d$ is not to be equated with $\tilde{\epsilon}_d$ but $\tilde{\epsilon}_d/z$. In the mixed valence regime $\epsilon_d + U \sim 0$ the Haldane shift can be seen to be in the opposite direction, to lower energies.

In the full and empty orbital regimes again the Hartree-Fock is a reasonable approximation, particularly when the effective level lies away from the Fermi-level, even though in this case we have a large value of U. With $\epsilon_d = -3\pi\Delta$, $U = 2\pi\Delta$, $n_d = 1.82$, the Hartree-Fock estimate of the position of the renormalized level $\tilde{\epsilon}_d/\pi\Delta = (\epsilon_d + Un_d/2)/\pi\Delta = -1.17$ is in good agreement with the renormalization group results, as can be seen in Figure 6. The fact that the quasiparticle interaction $\tilde{U}$ is compara-

tively large in the full and empty orbital regimes does not imply that the interaction effects on the low energy scale in these regimes are large. On the contrary they are small, as can be seen from the fact that R approaches unity in these two regimes. The reason is that the significant term is the combination $\tilde{U}\tilde{\rho}(0)$, and in these regimes $\tilde{\rho}(0) \to 0$ as the renormalized level moves well away the Fermi-level, such that $\tilde{U}\tilde{\rho}(0)$ is quite small. A similar situation applies in the case of the $U = \infty$ N-fold degenerate Anderson model where slave boson mean field theory is asymptotically exact in the limit $N \to \infty$. The mean field theory in that case is valid not because $\tilde{U} \to 0$ as $N \to \infty$, in fact $\tilde{U}$ remains finite in the limit, but because $\tilde{\rho}(0) \to 0$ so the combination $\tilde{U}\tilde{\rho}(0) \to 0$ as $N \to \infty$ [22].

Though we have derived a consistent picture in the form of a renormalized Anderson model to describe the low energy behaviour within both the NRG and RPT approaches, they differ in detail for calculations on higher energy scales. In the Wilson NRG approach further interaction terms are generated on higher energy scales, and the effective Hamiltonian for these energy scales no longer corresponds to a renormalized Anderson model. In contrast in the RPT approach, no higher order interaction terms have to be added and the Hamiltonian formally remains of the same. However, the counter terms have to be fully taken into account order by order in the expansion in $\tilde{U}$. Feynman diagrams corresponding to higher order in $\tilde{U}$ become increasingly important on higher energy scales, and are needed to describe the eventual 'undressing' of the fully renormalized quasiparticles. Calculations of this type to third order in $\tilde{U}$ have been carried out for the particle-hole symmetric model to determine corrections to the Fermi liquid regime [5].

3 Model with a coupling to phonons

One possible modification of the impurity model is the inclusion of an interaction with phonons. Such a term could be important when dealing with an impurity with a partially filled $4f$ shell, as there can be a change of the ionic volume of the order of 10% when an electron is removed or added to the $4f$ shell due to the adjustment of electrons in the outer d and s shells. The simplest type of interaction to consider is a coupling of the occupation of the d or f shells to an Einstein phonon of frequency ω_0, which is of the form used to study polaronic effects in a tight-binding model by Holstein [24]. If we add such a term to the Hamiltonian for the Anderson model we get the Anderson-Holstein model, which we have studied in earlier work [25]. The additional term has the form,

$$H_{\mathrm{e-ph}} = g\left(b^\dagger + b\right)\left(\sum_\sigma d_\sigma^\dagger d_\sigma - 1\right) + \omega_0 b^\dagger b, \qquad (27)$$

where b and $b^\dagger$ are creation and annihilation operators for the phonon modes and a linear coupling has been assumed with a coupling constant g. Some insight into the behaviour of this model can be obtained by performing

a displaced oscillator transformation, so that the transformed model takes the form,

$$H' = \hat{U}^{-1}H\hat{U} = \sum_{\sigma} \epsilon_{d,\text{eff}}d_{\sigma}^{\dagger}d_{\sigma} + U_{\text{eff}}n_{d\uparrow}n_{d\downarrow}$$

$$+ \sum_{k,\sigma} V_{\mathbf{k}}\left(e^{\frac{g}{\omega_0}(b^{\dagger}-b)}d_{\sigma}^{\dagger}c_{k\sigma} + e^{-\frac{g}{\omega_0}(b^{\dagger}-b)}c_{k\sigma}^{\dagger}d_{\sigma} \right)$$

$$+ \sum_{k\sigma} \epsilon_k c_{k\sigma}^{\dagger}c_{k\sigma} + \omega_0 b^{\dagger}b, \tag{28}$$

where

$$\hat{U} = e^{-\frac{g}{\omega_0}(b^{\dagger}-b)(\sum_{\sigma} n_{d,\sigma}-1)}, \tag{29}$$

and

$$\epsilon_{d,\text{eff}} = \epsilon_d + \frac{g^2}{\omega_0}, \quad U_{\text{eff}} = U - \frac{2g^2}{\omega_0}. \tag{30}$$

In the large frequency limit $\omega_0 \to \infty$, such that g^2/ω_0 remains finite, the model is equivalent to the original Anderson model with an effective level $\epsilon_{d,\text{eff}}$ and an effective local interaction U_{eff}, because in this limit the exponential terms that modify the hybridization term are equal to 1. When the original Coulomb interaction term $U = 0$, the effective interaction is attractive ($U_{\text{eff}} < 0$), so that in the localized strong coupling regime local bipolarons form, which is equivalent to the formation of a local moment in the spin model, and there is a Kondo effect in the charge (or equivalently isospin) channel.

For the large ω_0 limit, such that we can neglect the effect of the exponential terms in the hybridization in the Hamiltonian (28), we require ω_0 to be much greater than the conduction bandwidth D [26], which is unrealistic. For the regime $\omega_0 \ll D$, the physically appropriate one, the exponential terms in the phonon operators in (28) modify the form of the original Anderson model. Nevertheless the low energy fixed point, and the leading irrelevant interaction terms, should correspond to a renormalized Anderson model. The explicit inclusion of the phonon terms should only be necessary in considering higher order irrelevant terms, which contribute only at higher energy scales and higher temperatures. The derivation of the renormalized parameters in equation (2) holds provided that the self-energy $\Sigma(\omega)$ is analytic at $\omega = 0$. We can test this conjecture explicitly by again fitting the lower energy levels obtained in the NRG calculations to a renormalized Anderson model with parameters $\tilde{\epsilon}_d$, $\tilde{\Delta}$ and $\tilde{U}$. We first of all look at the results for the particle-hole symmetric model with $U = 0$, where the phonons induce a negative-U term, and assume particle-hole symmetry to compare our results with those obtained in the previous section. In the large ω_0 limit these will be identical to those obtained earlier with U being replaced by $U_{\text{eff}} = U - 2g^2/\omega_0$. For comparison we consider the results for a value of $\omega_0 \ll D$ and a commensurately smaller value of the coupling g, so that it covers a similar range of values of U_{eff}. The results of such a fitting, using the procedure outlined in the previous section, are shown in Figure 7 for $\omega_0/D = 0.05$, and for comparison also the case corresponding to $\omega_0 \to \infty$. These values cover the negative U_{eff} regime as we have $U = 0$. We
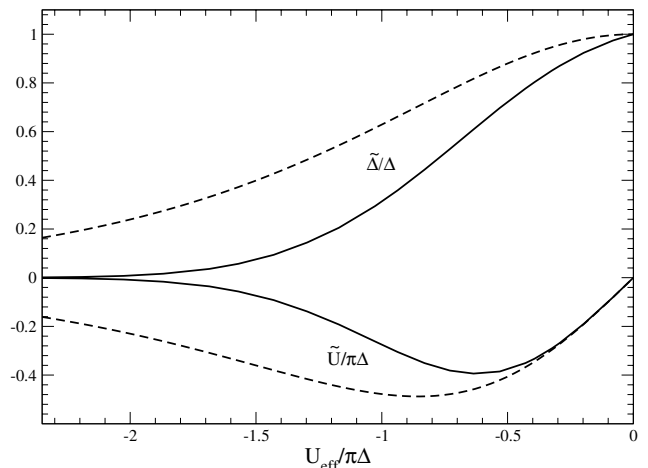

Fig. 7. The values of the renormalized parameters $\tilde{\Delta}/\Delta$ and $\tilde{U}/\Delta$ for the symmetric model with phonons ($U = 0$) plotted as a function of $U_{\text{eff}}/\pi\Delta = -2g^2/\omega_0\pi\Delta$. The dashed curves correspond to the limit $\omega_0 \to \infty$ (U_{eff} finite) and are the same as those for the negative-U model shown in Figure 2. The full lines are for the corresponding curves with $\omega_0 = 0.05$.
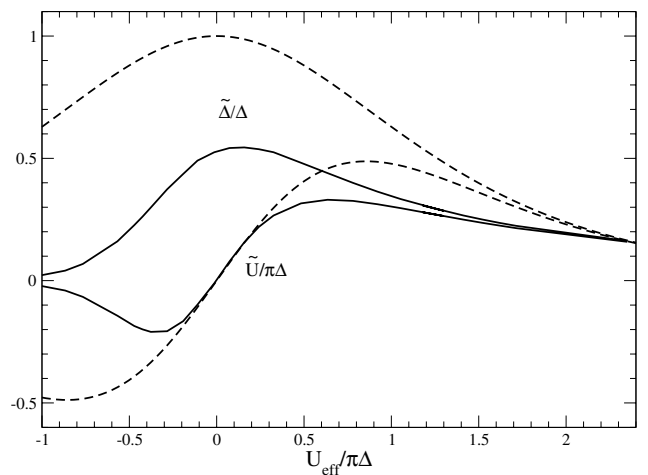

Fig. 8. The values of the renormalized parameters $\tilde{\Delta}/\Delta$ and $\tilde{U}/\Delta$ for the symmetric model with phonons, and $U/\pi\Delta = 2.35$, plotted as a function of $U_{\text{eff}}/\pi\Delta = (U - 2g^2/\omega_0)/\pi\Delta$. The dashed curves correspond to the limit $\omega_0 \to \infty$ (U_{eff} finite) and are the same as those for the pure Anderson model shown in Figure 2. The full lines are for the corresponding curves with $\omega_0 = 0.05$.

see that, as the coupling g increases, the values of $\tilde{\Delta}$ decrease much more rapidly in the smaller phonon frequency case than in the large ω_0 case due to the exponential terms that modify the hybridization in equation (28). The values of $\tilde{U}$ are also commensurately smaller because in the localized or local bipolaron limit, we must have $\tilde{U} = -\pi\tilde{\Delta}$, which is the case for both sets of results in the strong coupling limit.

In the results shown in Figure 8 we start with a value of $U/\pi\Delta = 2.35$ for which the impurity charge is almost localized and we are in the Kondo regime: as we increase g one effect is to decrease the value of U_{eff},
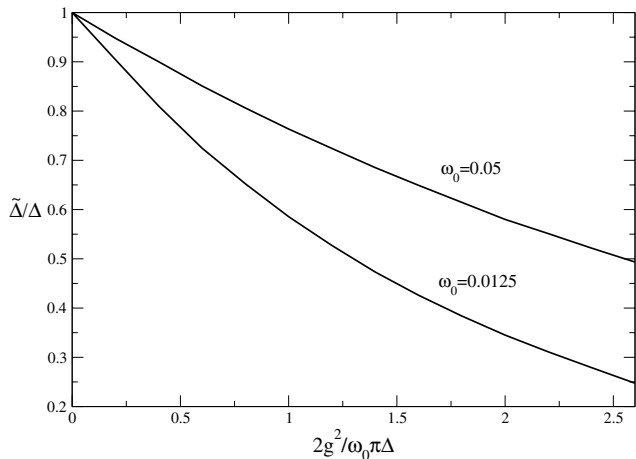
Fig. 9. A plot of the renormalized resonance width $\tilde{\Delta}/\Delta$ for the symmetric model with a phonon coupling g as a function of $2g^2/\omega_0\pi\Delta$ with values of U chosen such that $U_{\text{eff}} = U - 2g^2/\omega_0 = 0$, for the two cases $\omega_0 = 0.05$ and $\omega_0 = 0.0125$.

Fig. 10. The renormalized parameters, $\tilde{\Delta}/\pi\Delta$, $\tilde{\epsilon}_d/\pi\Delta$, and $\tilde{U}/\pi\Delta$, the Wilson ratio R and the impurity occupation value n_{imp} plotted for the asymmetric model ($U = 0$) with a coupling to phonons for a fixed value of $\epsilon_d = -\pi\Delta$ as a function of $U_{\text{eff}}/\pi\Delta$ for $\omega_0 = 0.05$.

and in the large ω_0 limit this is the sole effect, so that when $U_{\text{eff}} = 0$ we are left with an unrenormalized width parameter $\tilde{\Delta} = \Delta$. In the low ω_0 case the renormalized interaction $\tilde{U}$ changes sign at the same point as the bare parameter U_{eff} changes sign. This result is somewhat surprising. As the effective interaction induced by the phonons is only valid on the scale $\omega \ll \omega_0$, one might have expected that the on-site interaction U would be significantly renormalized on reducing the energy scale to $\omega \sim \omega_0$, say to $\bar{U}$, so that $\bar{U}$ would change sign when $\bar{U} = 2g^2/\omega_0$, which would be significantly shifted from the condition $U_{\text{eff}} = 0$. This is not the case which implies that both the direct and phonon induced interaction terms are renormalized in a similar way.

At the point where $\tilde{U} = 0$ there are polaronic effects, which are absent in the large ω_0 limit, such that $\tilde{\Delta}$ is significantly renormalized. For the values used here the width is reduced by factor of approximately 2 when $\tilde{U} = 0$. In the negative-U_{eff} regime the behaviour is as in Figure 7, with bipolaronic localization and $\tilde{U} = -\pi\tilde{\Delta}$, with very much reduced values of $\tilde{U}$ and $\tilde{\Delta}$ for the small frequency case as compared with the corresponding values for the large ω_0 limit.

In the corresponding spinless model with a coupling to phonons there is no induced attractive on-site interaction, but polaronic effects occur due to the retarded effective potential [24]. In the model with spins, we can reveal these polaronic effects if we choose values of U which cancel the attractive interaction that leads to bipolaron formation, $U_{\text{eff}} = U - 2g^2/\omega_0 = 0$. We look at the renormalized resonance width for the symmetric model for a range of values of the electron-phonon coupling g with appropriately chosen values of U. As a consequence the renormalized quasiparticle interaction $\tilde{U}$ is negligible. The results for the symmetric model are shown in Figure 9 for $\omega_0 = 0.05$ and $\omega_0 = 0.0125$ ($D = 1$). It can be seen that the decrease in $\tilde{\Delta}$ with increase of g is greater in the smaller phonon frequency case. In the
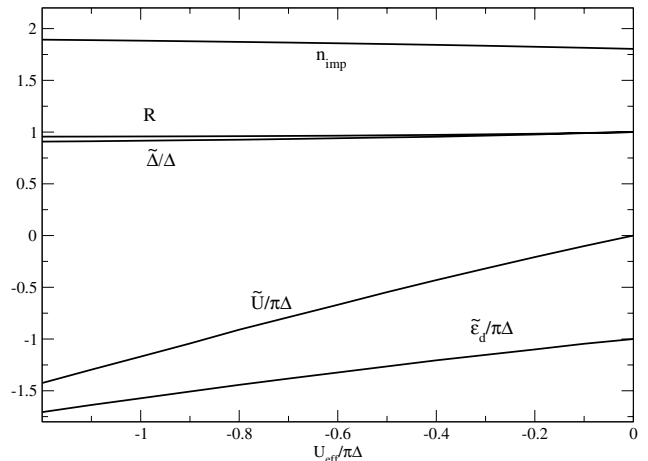
limiting case $\omega_0 \rightarrow \infty$ ($2g^2/\omega_0$ finite) there is no polaronic effect and $\tilde{\Delta}/\Delta = 1$ in all cases. Some insight into the behaviour of the asymmetric model ($U = 0$) with a coupling to phonons can be gained by comparing with the negative-U_{eff} Anderson model as it corresponds to the case $\omega_0 \rightarrow \infty$. The asymmetric model with negative-U can be mapped into a positive-U symmetric model with a finite magnetic field $H \sim -\epsilon_d$ under the interchange of charge and spin; the one-electron spectral density for the isospin up electrons is given by $\rho_d(\omega)$ and that for the isospin down by $\rho_d(-\omega)$. A finite ϵ_d favours either the doubly occupied state (isospin up) for $\epsilon_d < 0$, or the empty state for $\epsilon_d > 0$, so that increasing the value of $|U_{\text{eff}}|$ has the effect of further increasing the polarization. The results for the renormalized parameters for the asymmetric model with phonons ($U = 0$ and $\epsilon_d = -\pi\Delta$) and finite ω_0 ($= 0.05$) which are plotted in Figure 10 show a similar trend. As g^2 increases, or equivalently U_{eff} decreases, both $\tilde{\epsilon}_d$ and $\tilde{U}$ decrease linearly, and the occupation of the impurity level slowly increases and tends to the value 2. The interaction effects on the low energy behaviour can be seen to be relatively small because, as $\tilde{\epsilon}_d$ moves further from the Fermi-level, the quasiparticle density of states at Fermi-level $\tilde{\rho}_d(0)$ decreases and $R \sim 1$. This trend can be clearly seen in the calculated values of the spectral density $\rho_d(\omega)$ [25], and $\tilde{\epsilon}_d$ tracks the peak in $\rho_d(\omega)$. The peaks in $\rho_d(\omega)$ become asymmetric for strong electron-phonon coupling, as phonon side-bands excitations are induced on the low energy side of the peak, giving the appearance of a broadened peak. The peak of the renormalized Anderson peak, however, is symmetric with a width $\tilde{\Delta}$ slightly reduced from the bare value Δ, but is quite compatible with the spectra seen in $\rho_d(\omega)$ for small ω. The renormalized model has to reproduce the quasiparticle spectrum only in the immediate neighbourhood of the Fermi-level which in this case lies on the higher energy side of the peak in $\rho_d(\omega)$.

4 Model with a Falikov-Kimball interaction

Apart from the interaction U between the electrons in the local d- or f-orbitals at the impurity site there will also be a two-body interaction between the electrons in these orbitals and the conduction electrons. Such a term does not appear in the standard Anderson model but a local interaction of this type is included in the Falikov-Kimball model [27]. It is the sole two-body interaction term in this model, which was put forward as an appropriate model for investigating valence instabilities in compounds, where the occupation of the localized f-orbitals changes significantly as a result of pressure or alloying (see reference [28] for a recent review). The reason that it is not usually included in impurity models, is not because the interaction is very small, but because it is thought not to play an essential role in understanding the impurity behaviour. This means that its effects can, for the most part, be absorbed as a renormalization of terms that are already within the standard models. We can put this hypothesis to the test by including such a term in the Hamiltonian and then consider what effect it has on the renormalized parameters of the low energy fixed point. In the discrete linear chain version of the Anderson model, equation (11), used in the NRG calculations such a term can be included as an interaction between the impurity and the electron occupation at the first site on the conduction electron chain,

$$H_{\mathrm{FK}} = U_{\mathrm{fk}} \sum_{\sigma,\sigma'} n_{d,\sigma} n_{0,\sigma'}, \tag{31}$$

where U_{fk} denotes the matrix element of the interaction. We add this term to the Hamiltonian in equation (11) and then examine the nature of the low energy fixed point. We take $U = 2\pi\Delta$, as earlier, with $U_{\mathrm{fk}} = U/2 = \pi\Delta$, and take a range of values of ϵ_d to run from the full orbital, through the Kondo, to the empty orbital regime. We can then compare the results with those obtained from a similar study in Section 3.

The results for the renormalized parameters in this study are shown in Figure 11. The low temperature behaviour of the model, $\chi_{\mathrm{s,imp}}$, $\chi_{\mathrm{c,imp}}$ and γ_{imp}, can be deduced by substituting the renormalized parameters into equations (6) and (8). There is a clear correspondence with results derived earlier for the Anderson model without this additional term, shown in Figure 6. To examine the correspondence in more detail we have replotted the values from Figure 6 in the same figure, using dotted lines, and have displaced the curves by a constant shift of $\pi\Delta = U_{\mathrm{fk}}$, such that the original bare level ϵ_d from Figure 6 is replaced by an effective bare level $\bar{\epsilon}_d = \epsilon_d + U_{\mathrm{fk}}$. The agreement between the results with the additional Falikov-Kimball term, $U_{\mathrm{fk}} = \pi\Delta$, and those of the model with $U_{\mathrm{fk}} = 0$ and an effective bare level $\bar{\epsilon}_d$ are quite remarkable. In the strong correlation regime the differences are less than 5%, and overall less than 10%. As the nature of the low energy fixed point has not been changed by the inclusion of the Falikov-Kimball term, it is not surprising that the low energy behaviour can still be described by a renormalized Anderson model. What is somewhat unexpected in this case is that these renormalized parameters
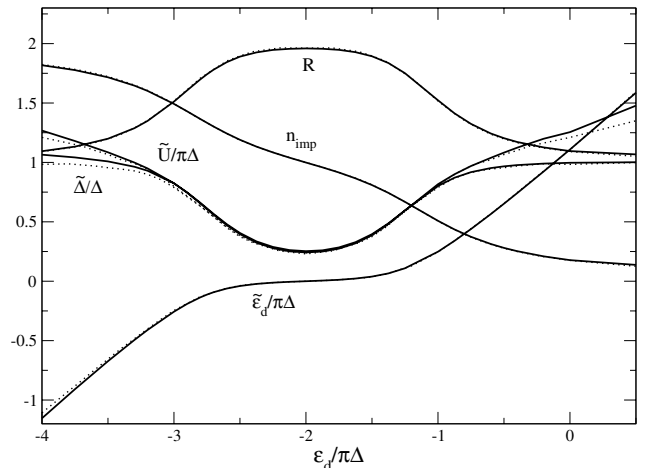

Fig. 11. The renormalized parameters $\tilde{\Delta}/\pi\Delta$, $\tilde{\epsilon}_d/\pi\Delta$, and $\tilde{U}/\pi\Delta$, the Wilson ratio R and the impurity occupation value n_{imp} are plotted for the Anderson model with an additional Falikov-Kimball interaction U_{fk}. The values of U and U_{fk} are fixed, such that $U_{\mathrm{fk}} = U/2 = \pi\Delta$, and $\epsilon_d/\pi\Delta$ is varied over the range indicated. Also shown as dotted curves are the renormalized values for the Anderson model with $U_{\mathrm{fk}} = 0$, corresponding to those shown in Figure 6, but with a shift of ϵ_d such that $\epsilon_d \rightarrow \epsilon_d - U_{\mathrm{fk}}$. There is a remarkable agreement with these displaced results over this range.

correspond to a constant shift of the bare level over the whole parameter range, and that no adjustment of the bare hybridization term is required.

To examine whether this shift varies or not with U, we take $\epsilon_d = -2\pi\Delta$ with $U_{\mathrm{fk}} = \pi\Delta$ so that $\epsilon_d + U_{\mathrm{fk}} = -\pi\Delta$, and vary U over the same range as in the results for the pure Anderson model shown in Figure 4. If the effective bare level $\bar{\epsilon}_d$ is independent of U the results should coincide with those shown in Figure 4. The results of these calculations are shown in Figure 12. Again we see that the results are close to those of the Anderson model without this term, with the same shift in the bare ϵ_d. The difference in values are less than 4% for $U/\pi\Delta > 1$, and less than 12% overall. In these results, and those shown in Figure 11, the differences in the values of n_{imp} are even smaller, less than 1%, over the whole parameter range.

We conclude that the low temperature behaviour of the model with a Falikov-Kimball interaction U_{fk} in this parameter regime is very similar to that of an Anderson model without this term, but with a shift of ϵ_d to $\bar{\epsilon}_d = \epsilon_d + U_{\mathrm{fk}}$. The shift is approximately independent of ϵ_d and U, and linear for U_{fk} in the range $0 < U_{\mathrm{fk}}/\pi\Delta < 2.0$. In this range we found the deviations between the results of the effective model with $\bar{\epsilon}_d$ and the model with the Falikov-Kimball term increase linearly with the value of U_{fk}.

In the case of a vanishing hybridization the nature of the fixed point Falikov-Kimball term will be different as it will correspond to an X-ray type of problem, with the localized impurity electron corresponding to a core-hole, and the self-energy at $\omega = 0$ will be singular [29]. This, however, is a special case, and in general we can expect
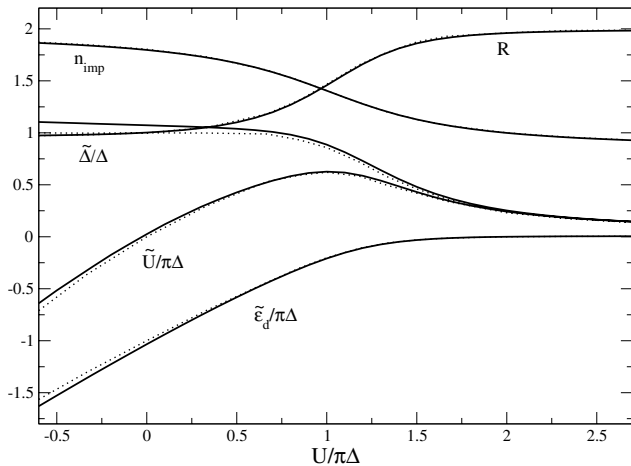
Fig. 12. The renormalized parameters $\tilde{\Delta}/\pi\Delta$, $\tilde{\epsilon}_d/\pi\Delta$, and $\tilde{U}/\pi\Delta$, the Wilson ratio R and the impurity occupation value $n_{\rm imp}$ for the Anderson model with an additional Falikov-Kimball interaction $U_{\rm fk}$, using the same value as for Figure 11. Here, $\epsilon_d = -2\pi\Delta$, and $U/\pi\Delta$ is varied over the range indicated. These results are compared with the corresponding values for the Anderson model with $U_{\rm fk} = 0$ (dotted curves) shown in Figure 4, for which $\epsilon_d = -\pi\Delta$. There is again a close agreement with the results of the model without the additional term but with a displaced ϵ_d.

the self-energy to be regular at $\omega = 0$ and the renormalized Anderson model to provide the appropriate low energy model (see also the discussion in Sect. V. B of reference [28]).

5 Conclusions

We have shown explicitly that in all parameter regimes the low energy behaviour of the Anderson model can described by the same Anderson impurity model but with renormalized parameters. We have also presented a new and efficient way of calculating these parameters using the NRG. The combination of the NRG and RPT techniques gives a very simple and accurate way of calculating the low temperature properties of the model: the NRG is used to estimate the parameters, which are then substituted into the RPT expressions for the thermodynamics and response functions. This procedure, is a much simpler than the original NRG approach [1,2], and avoids the numerical problems in subtracting off the conduction electron component.

The Anderson model, as a model for impurity systems, neglects many higher energy scale interactions. In including an electron-phonon coupling and a Falikov-Kimball term we have included some of the possible higher energy interaction terms. Explicit calculations given here have shown that these terms do not change any essential features of the low energy behaviour, which can still be described in terms of a three-parameter renormalized Anderson model, though the renormalized parameters are modified. It is reasonable to assume that if other types

of interaction terms are included, such as two-body hybridization terms arising from off-diagonal elements of the Coulomb interaction of the impurity d-electron with the conduction electrons, that the same would hold. The fact that we can describe the various forms of low energy behaviour of this class of non-degenerate impurity models, within the framework of a single renormalized model, gives a unifying perspective. It also simplifies the interpretation of experiments on the low temperature behaviour of impurity systems if the results can be analysed in terms of a single three-parameter model.

On higher energy scales some of these extra interactions may have to be taken into account explicitly, while in other cases they can be absorbed into the parameters of the bare model. For example, in the model with a coupling to phonons, for $\omega_0 \to \infty$ the virtual interaction terms due to the phonons can be simply absorbed as modifications of the bare parameters $\bar{\epsilon}_d$ and $\bar{U}$, while for energy scales $\omega > \omega_0$ they have to be included explicitly. Even the terms that are included explicitly in the Anderson model are to a degree already renormalized. The interaction term U of the bare Anderson model does not correspond to the Coulomb matrix elements for electrons in localized d-orbitals, but is an effective parameter which takes into account the many-body relaxation and screening effects of the other electronic shells, when a d or f-electron is removed. This is true for most bare models: which interactions have to be taken into account explicitly is dependent on the energy scales and the type of experiment which is being described.

Appendix A

Let the linear chain Hamiltonian (11) of the non-interacting system plus impurity be denoted by $H_{-1,N}^0$, and that of the rest of the chain without the impurity starting at site i by $H_{i,N}^0$, where $i = 0, 1, 2 \ldots$. We are considering free single particle excitations for $\tilde{U} = 0$ so that the Green's function at the impurity site ($i = -1$) is given by

$$G_{-1-1}(\omega) = \frac{1}{\omega - \epsilon_d \Lambda^{(N-1)/2} - V^2 \Lambda^{(N-1)} g_{00}(\omega)} \quad (32)$$

where $g_{00}(\omega)$ is the Green's function at site $i = 0$ for the system described by the Hamiltonian $H_{0,N}^0$. This Green's function is given in turn by

$$g_{00}(\omega) = \frac{1}{\omega - \xi_0^2 \Lambda^{(N-1)} g_{11}(\omega)} \quad (33)$$

and $g_{11}(\omega)$ is the Green's function at site $i = 1$ for the system described by the Hamiltonian $H_{1,N}^0$. This procedure can be extended to express $g_{00}(E)$ in the form of a continued fraction.

The one-particle excitations E are given by the poles of (32),

$$E - \epsilon_d \Lambda^{(N-1)/2} - V^2 \Lambda^{(N-1)} g_{00}(E) = 0, \qquad (34)$$

where $g_{00}(E)$ can be expressed in the form,

$$g_{00}(E) = \sum_{l=1,N+1} \frac{|\phi_l(0)|^2}{E - \tilde{E}_l(N)}, \qquad (35)$$

where $\phi_l(0)$ and $\tilde{E}_l(N)$ are the eigenvectors and eigenvalues of $H_{0,N}^0$.

If $E_p^0(N)$ and $E_h^0(N)$ are the lowest particle and hole excitations from the ground state of the Hamiltonian $H_{-1,N}^0$ then,

$$\frac{E_p^0(N)\Lambda^{-(N-1)/2}}{V^2} - \frac{\epsilon_d}{V^2} = \Lambda^{(N-1)/2} g_{00}\left(E_p^0(N)\right), \quad (36)$$

$$\frac{-E_h^0(N)\Lambda^{-(N-1)/2}}{V^2} - \frac{\epsilon_d}{V^2} = \Lambda^{(N-1)/2} g_{00}\left(-E_h^0(N)\right). \qquad (37)$$

If we replace $E_{p(h)}^0$ by the corresponding values for the interacting system $U \neq 0$, $E_{p(h)}$, then they can be used to define N-dependent quantities, $\tilde{\epsilon}_d(N)$, and $\tilde{\Delta}(N) = \pi \tilde{V}(N)^2/2$,

$$\frac{\pi E_p(N)\Lambda^{-(N-1)/2}}{2\tilde{\Delta}(N)} - \frac{\pi \tilde{\epsilon}_d(N)}{2\tilde{\Delta}(N)} = \Lambda^{(N-1)/2} g_{00}(E_p(N)), \qquad (38)$$

$$\frac{-\pi E_h(N)\Lambda^{-(N-1)/2}}{2\tilde{\Delta}(N)} - \frac{\pi \tilde{\epsilon}_d(N)}{2\tilde{\Delta}(N)} = \Lambda^{(N-1)/2} g_{00}(-E_h(N)). \qquad (39)$$

The renormalized parameters $\tilde{\epsilon}_d$ and $\tilde{\Delta}$ corresponding to the low energy fixed point are given by $\tilde{\epsilon}_d = \lim_{N\to\infty} \tilde{\epsilon}_d(N)$ and $\tilde{\Delta} = \lim_{N\to\infty} \tilde{\Delta}(N)$, and are determined by the two equations,

$$\frac{\pi \tilde{\epsilon}_d}{2\tilde{\Delta}} = \lim_{N\to\infty} \Lambda^{(N-1)/2} g_{00}(\pm E_{p(h)}(N)), \qquad (40)$$

and

$$\frac{\pi}{2\tilde{\Delta}} = \lim_{N\to\infty} \frac{\Lambda^{(N-1)}(g_{00}(E_p(N)) - g_{00}(-E_h(N)))}{E_p(N) + E_h(N)}. \qquad (41)$$

The results in equations (40) and (41) are applicable also to systems with non-symmetric or non-constant densities of conduction states, with the appropriate form for $g_{00}(\omega)$, which can be evaluated using either equation (35) or (33).

References

1. K.G. Wilson, Rev. Mod. Phys. **47**, 773 (1975)
2. H.R. Krishnamurthy, J.W. Wilkins, K.G. Wilson, Phys. Rev. B **21**, 1003 and 1044 (1980)
3. See for example, N.N. Bogoliubov, D.V. Shirkov, *Introduction to the Theory of Quantized Fields* (Wiley-Interscience, New York, 1980)
4. A.C. Hewson, Phys. Rev. Lett. **70**, 4007 (1993)
5. A.C. Hewson, J. Phys.: Condens. Matter **13**, 10011 (2001)
6. P.W. Anderson, Phys. Rev. **124**, 41 (1961)
7. D.M. Newns, A.C. Hewson, J. Phys. F **10**, 2429 (1980)
8. That these results are exact can be deduced from a Ward identity. For details see references [10,4]
9. J. Friedel, Can. J. Phys. **54**, 1190 (1956); J.M. Langer, V. Ambegaokar, Phys. Rev. **164**, 498 (1961); D.C. Langreth, Phys. Rev. **150**, 516 (1966)
10. K. Yamada, Prog. Theor. Phys. **53**, 1970 (1975); **54**, 316 (1975)
11. P. Nozières, J. Low Temp. Phys. **17**, 31 (1974): *Low Temperature Physics Conference Proceedings LT14*
12. A. Oguri, Phys. Rev. B **64**, 153305 (2001)
13. A.M. Tsvelick, P.B. Wiegmann, Adv. Phys. **32**, (1983)
14. B. Horvatić, V. Zlatić, J. Phys. France **46**, 1459 (1985)
15. A.C. Hewson, J. Phys.: Condens. Matter **5**, 6277 (1993)
16. J. Rasul, A.C. Hewson, J. Phys. C **17**, 3337 (1984)
17. G.M. Falco, R.A. Duine, H.T.C. Stoof, `cond-mat/0304489` (2003)
18. O. Sakai, Y. Shimizu, T. Kasuya, Prog. Theor. Phys. Suppl. **108**, 73 (1992)
19. O. Sakai, Y. Shimizu, T. Kasuya, J. Phys. Soc. Jpn **58**, 3666 (1989)
20. T.A. Costi, A.C. Hewson, V. Zlatić, J. Phys.: Condens. Matter **6**, 2519 (1994)
21. F.M.D. Haldane, Phys. Rev. Lett. **40**, 416 (1978)
22. A.C. Hewson, *The Kondo Problem to Heavy Fermions*, Chap. 7 (Cambridge Univ. Press, Cambridge, 1993 and 1997)
23. This is a feature of the discrete model, more generally in a continuum case one might expect these terms to fall off as $1/N$
24. T. Holstein, Ann. Phys. Lpz. **8**, 325 (1959)
25. A.C. Hewson, D. Meyer, J. Phys. Condens. Matter **14**, 427 (2002)
26. D. Meyer, A.C. Hewson, Acta Physica Polonica B **34**, 769 (2003)
27. L.M. Falikov, J.C. Kimball, Phys. Rev. Lett. **22**, 997 (1969)
28. J.K. Freericks, V. Zlatić, Rev. Mod. Phys. **75**, 1333 (2003)
29. G.D. Mahan, *Many Particle Physics* (Plenum, New York, 1990)